



Investigation of the Effects of Immersion Period of Simulated Body Fluid on the Morphology and Structural Properties of Fe/Ni co-Doped Chlorapatites

Serhat Keser^{1,*}, Tankut Ates², Niyazi Bulut³, Omer Kaygılı³

¹Department of Chemical Technology, EOSB Vocational School, Firat University, 23119, Elazig, Türkiye

²Department of Engineering Basic Sciences, Faculty of Engineering and Natural Sciences, Malatya Turgut Özal University, Battalgazi, Malatya, Türkiye

³Department of Physics, Faculty of Science, Firat University, 23119, Elazig, Türkiye

*Corresponding author: Serhat Keser email: serhatkeser@gmail.com

ABSTRACT

In this study, chlorapatite (ClAp) samples co-doped with Fe and Ni at different amounts were synthesized using a wet chemical method. The as-produced samples were immersed in simulated body fluid (SBF) for 14 and 28 days. The samples were characterized before and after soaking in SBF, and their morphologies and structural properties were compared to each other. It was observed that the immersion period in SBF and the amount of Fe and Ni affected the morphology and structural properties of the ClAp samples.

ARTICLE INFO

Keywords:

Chlorapatite
Fe-doping
Ni-doping
SBF

Received: 2023-11-24

Accepted: 2023-11-30

ISSN: 2651-3080

DOI: 10.54565/jphcfum.1395724

1. Introduction

Apatites located among calcium phosphate ceramics have the general formula $\text{Ca}_{10}(\text{PO}_4)_6\text{X}_2$ and they are divided into three groups: *i*) Fluorapatites (FAp), *ii*) Chlorapatites (ClAp) and *iii*) Hydroxyapatites (HAp). In place of X in the general formula; if there is an F^- ion, this is called fluorapatite, if there is a Cl^- ion, this is called chlorapatite, and if there is an OH^- ion, this is called hydroxyapatite. The lattice structure of apatites can allow rare earth elements and transition metal ions to be incorporated into the structure. Many elements can be doped to the apatite structure instead of Ca by using chemical synthesis. During the doping process, the general stability and crystal structure of apatite can remain intact. ClAp is an important compound of apatites and has two polymorphous phases. The monoclinic phase with space group P21/b is produced at low temperatures and the typical hexagonal phase with space group P6₃/m is produced by heat treatment at temperatures above 350 °C [1,2]. The size, distribution and structural morphology properties of ClAp crystals can be controlled by some parameters such as elements and compounds added to the structure, synthesis temperature and method, etc. during the synthesis stage [3].

When the literature on ClAps is examined, Keochaiyom et al. [2] reported that the Fe-doped magnetic ClAp nanoparticles could remove heavy metals such as Zn^{2+} ,

Cd^{2+} and Pb^{2+} from aqueous solutions, and Han et al. [4] showed that the ClAp samples produced with the green synthesis method can be used successfully as an adsorbent in the treatment of Cr^{4+} from wastewater. In another study, Durugkar et al. [5] observed that the Eu^{3+} doped ClAp samples turned into white light LED when combined with blue LED. In addition to all these studies, Nasiri-Tabrizi et al. [6] Ta-doped, Wan et al. [7] sodium dodecyl sulfate (SDS) doped, Wan et al. [8] rhamnolipid doped, Subramanian et al. [9] Li-doped Sr-ClAp, Zhai et al. [10] Ba-ClAp, Rout and Agrawal [11] Gd^{3+} doped, Yuan et al. [12] Cd^{2+} -doped ClAp samples synthesized and tried to determine their various physical-chemical properties. The aim of this study is to determine the crystal structure, functional groups, morphology and structural changes in the simulated body fluid (SBF) of Fe/Ni-doped ClAp samples produced by the wet chemical method.

2. Materials and methods

As the starting reagents, calcium chloride (CC), iron (III) nitrate nonahydrate (IN), nickel (II) nitrate hexahydrate (NN) and diammonium hydrogen phosphate (DAP), purchased from the Sigma-Aldrich, were used in the preparation of chlorapatite samples. The first solution with a total volume of 100 mL of (50-x-y) mmol of CC, x mmol IN and y mmol NN was prepared. Where the x and y

values were selected as the same value for each sample. The $x=y$ values of 0.275, 0.550, and 0.825 were used for the synthesis of the 0.55Fe0.55NiClAp, 1.10Fe1.10NiClAp, and 1.65Fe1.65NiClAp samples, respectively. The second solution having a total volume of 100 mL of 30 mmol DAP was prepared. The first solution was poured into a beaker, and the second one was poured drop by drop into this. The final solution was stirred at 75 °C for 120 min, and then put into an oven at 190 °C for 15 h. The as-obtained powders were calcined in an electrical furnace at 825 °C for 2 h.

Each sample was divided into three equal portions. The first portion was preserved as is, while the second and third portions were subjected to simulated body fluid (SBF) using Kokubo's recipe [13] for 14 and 28 days, respectively. Before immersing in SBF, the second and third portions of the samples were converted to the pellets having a thickness of 3 mm and diameter of 12 mm under the pressure of 10 MPa. The as-pelleted samples were put into glass beakers containing 100 mL of SBF in an oven at 36.5 °C. SBF solutions in the beakers were renewed every second day. After 14 and 28 days of immersion, the samples were filtered, washed with distilled water three times and dried.

X-ray diffraction (XRD) measurements were taken using a Rigaku Rad B-DMAX II diffractometer. Fourier transform infrared (FTIR) spectra were collected by a PerkinElmer Spectrum One spectrophotometer using the KBr pellets. A ZEISS EVO 50 scanning electron microscope was used to perform the morphological investigations. All the experimental analyses were taken for the samples before and after SBF for 14 and 28 days.

3. Results

3.1. XRD results

Fig. 1 shows the XRD patterns of the samples before and after immersing in SBF for 14 and 28 days. The XRD patterns are matched with the ClAp (JCPDS pdf no 72-0010) with an orthorhombic crystal structure for all the samples. The formation of the same phase as a single phase was observed by Yu et al. [14] for the samples calcined at 800 °C. The amount of the contents and immersion period in SBF affect the intensities of the peaks and cause the shifts in the peak positions.

To estimate the crystallite size (D), the following Scherrer equation was used [15]:

$$D = \frac{0.9\lambda}{\beta \cos \theta} \quad (1)$$

It is seen that the D values given in Table 1 were affected by the duration of SBF and amount of the co-dopants as used.

The lattice parameters (a , b and c) and unit cell volume of the ClAp samples co-doped with Fe and Ni were computed using the following relations belonging to the orthorhombic crystal structure [16].

$$\frac{1}{d^2} = \frac{h^2}{a^2} + \frac{k^2}{b^2} + \frac{l^2}{c^2} \quad (2)$$

$$V = a.b.c \quad (3)$$

By evaluating the values in Table 1, it can be seen that the immersion period in SBF and amount of Fe and Ni affect significantly the lattice parameters and volume of the unit cell of the ClAp structure.

3.2. FTIR results

Fig. 2 illustrates the FTIR spectra of the Fe/Ni co-doped ClAp samples before and after immersing in SBF for durations of 14 and 28 days. The phosphate group-related bands were detected at 1046, 726, 602 and 537 cm^{-1} [17]. The band observed at 1384 cm^{-1} can be associated with the carbonate group [18]. The bands centered at 3466 and 1640 cm^{-1} are assigned to the adsorbed water [19]. Similar to the XRD results, the composition and immersion time caused some shifts and changes in the intensity of the as-observed bands were detected in the FTIR measurements taken before and after soaking in SBF.

3.3. Morphological investigations

Fig. 3 shows the SEM images of the Fe/Ni co-doped ClAp samples before and after soaking in SBF for 14 and 28 days. The morphology is affected by the composition and duration of soaking. The as-observed variations in the morphology support the as-observed changes in the crystal structure-related parameters calculated from the XRD data.

4. Conclusions

In the present study, the structural properties and morphology of the ClAp samples co-doped with Fe and Ni at various amounts before and after immersing in SBF for 14 and 28 days were investigated in more detail. For all the samples, the formation of the single phase of the ClAp having the orthorhombic crystal structure was observed. The amount of the co-dopants of Fe and Ni affected the crystal structure-related parameters. These parameters were also affected by the duration of SBF. FTIR spectra also confirmed the formation of the apatitic structure. The amount of both co-dopants and soaking in SBF for the different periods caused some variations in the morphology. We think that the results of this study will make significant contributions to studies in the field of ClAp.

Table 1. The XRD analysis results before and after immersing in SBF

	Sample	<i>a</i> (nm)	<i>b</i> (nm)	<i>c</i> (nm)	<i>V</i> (nm) ³	<i>D</i> (nm)
Before SBF	0.55Fe0.55NiClAp	0.6191	0.6942	1.0823	0.4651	38.54
	1.10Fe1.10NiClAp	0.6208	0.6942	1.0817	0.4661	40.22
	1.65Fe1.65NiClAp	0.6079	0.6982	1.0817	0.4591	37.49
After SBF for 14 days	0.55Fe0.55NiClAp	0.6199	0.6939	1.0636	0.4575	39.83
	1.10Fe1.10NiClAp	0.6199	0.6933	1.0464	0.4497	38.72
	1.65Fe1.65NiClAp	0.6195	0.6922	1.0664	0.4573	38.36
After SBF for 28 days	0.55Fe0.55NiClAp	0.6191	0.6930	1.0618	0.4555	40.83
	1.10Fe1.10NiClAp	0.6195	0.6946	1.0792	0.4644	35.87
	1.65Fe1.65NiClAp	0.6186	0.6980	1.0611	0.4582	36.98

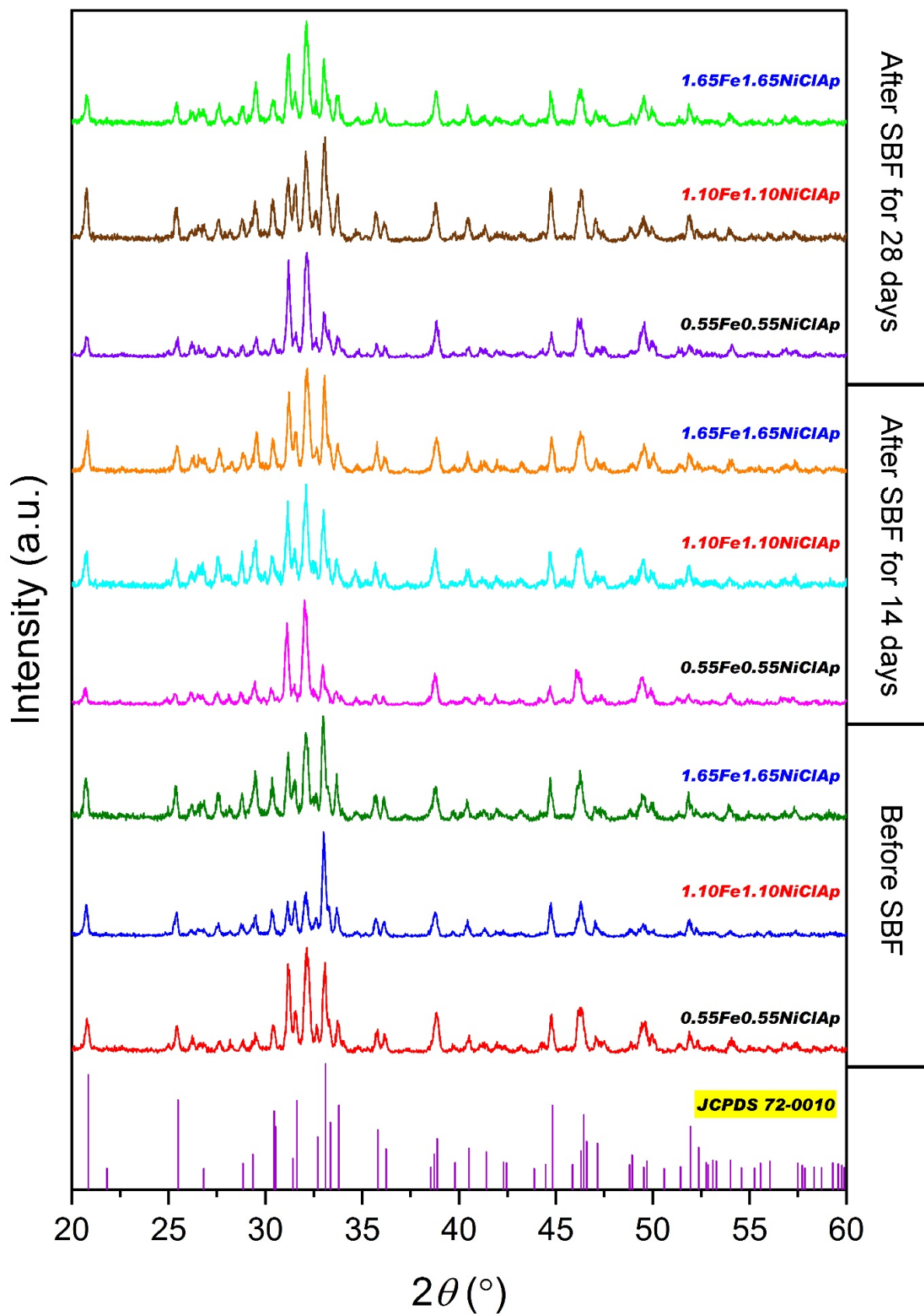


Fig. 1. XRD results of the samples

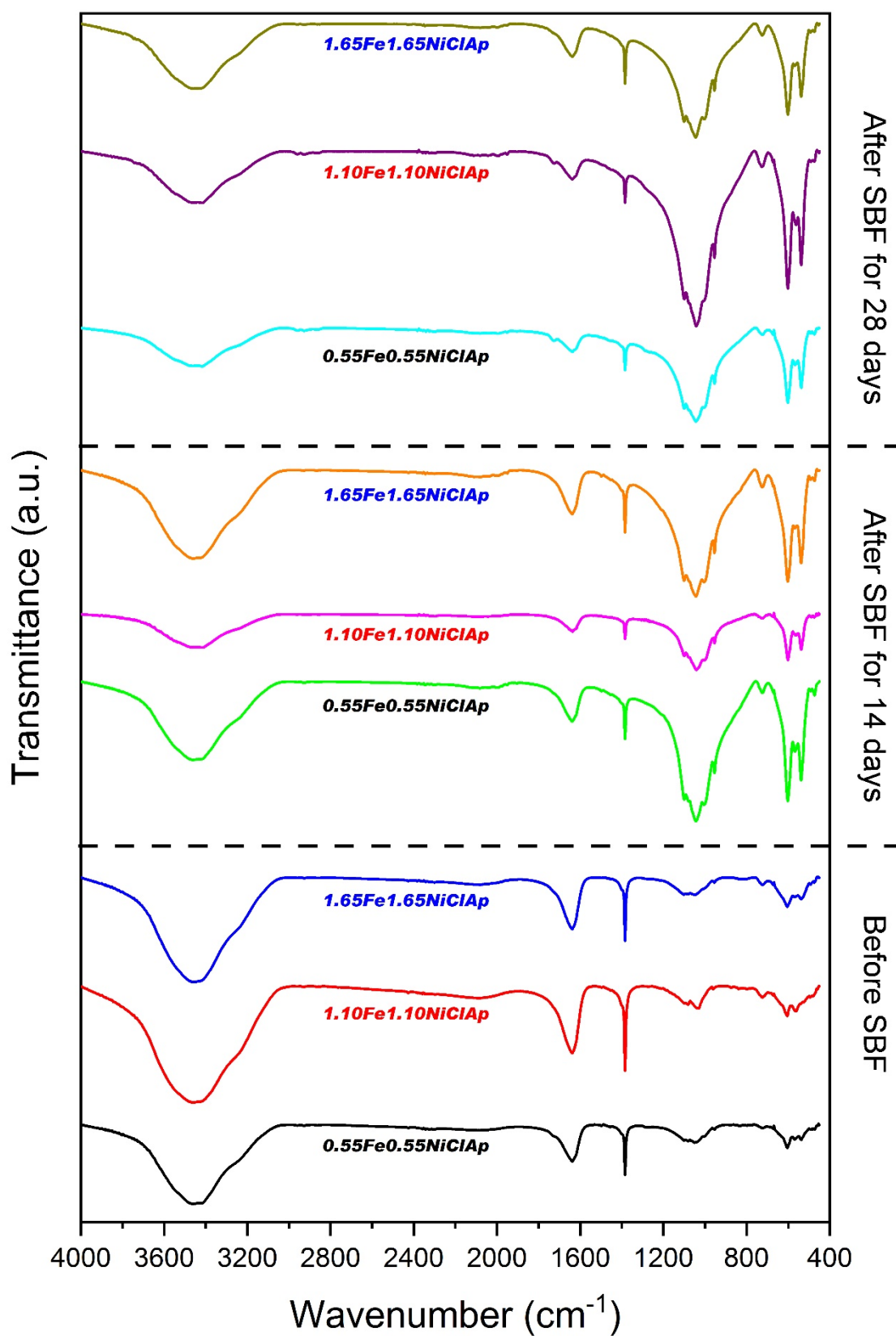


Fig. 2. FTIR results

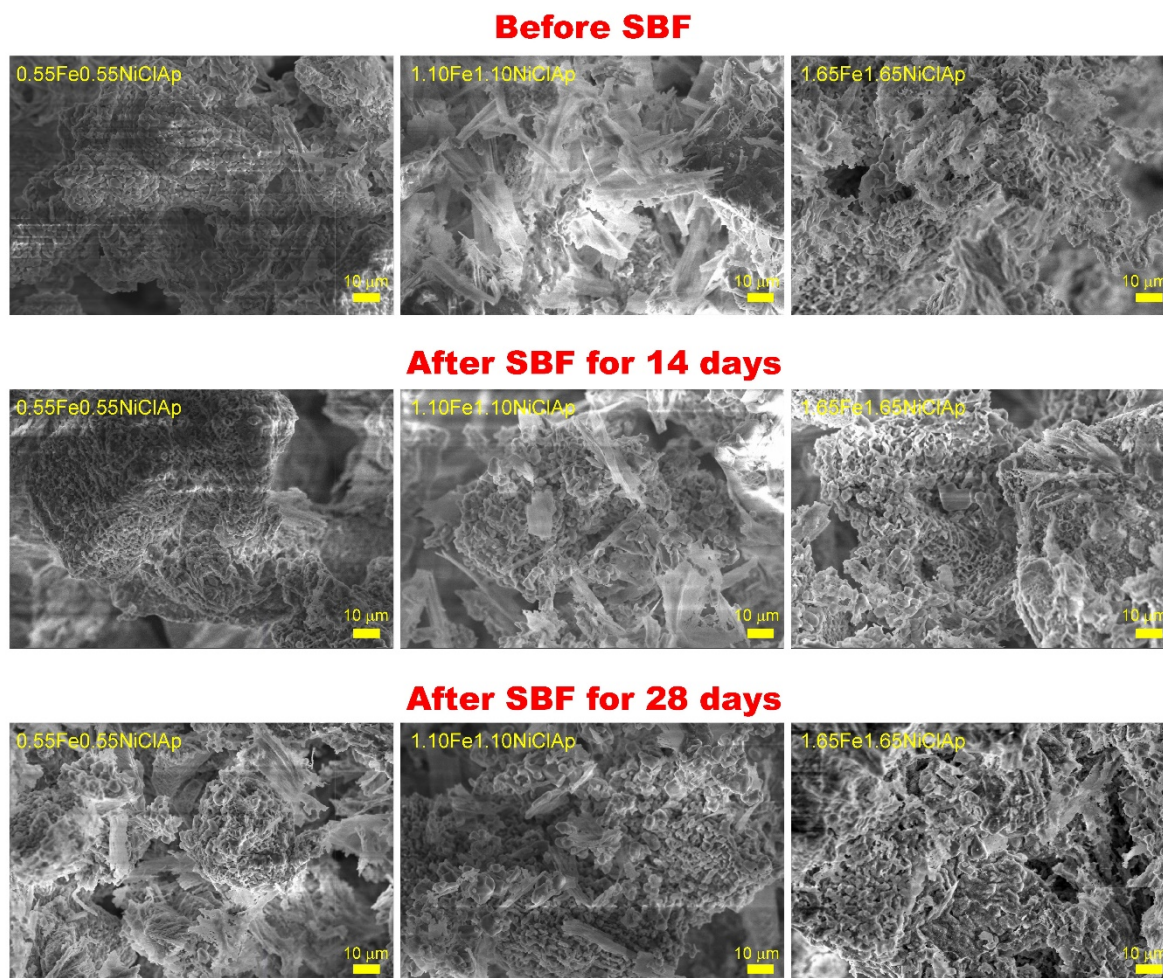


Fig. 3. SEM images of the ClAp samples before and after immersion in SBF for 14 and 28 days

References

- [1] H.P. Wu, C. Lai, G.M. Zeng, J. Liang, J. Chen, J.J. Xu, J. Dai, X.D. Li, J.F. Liu, M. Chen, L.H. Lu, L. Hu, J. Wan, "The interactions of composting and biochar and their implications for soil amendment and pollution remediation: a review" *Critical Reviews in Biotechnology*, 1-11, 2016.
- [2] B. Keochaiyom, J. Wan, G. Zeng, D. Huang, W. Xue, L. Hu, C. Huang, C. Zhang, M. Cheng, "Synthesis and application of magnetic chlorapatite nanoparticles for zinc (II), cadmium (II) and lead (II) removal from water solutions" *Journal of Colloid and Interface Science*, 505, 824-835, 2017.
- [3] M. Ganjali, S. Pourhashem, M. Mozafari, "The effect of heat-treatment on the structural characteristics of nanocrystalline chlorapatite particles synthesized via an in situ wet-chemical route" *Ceramics International*, 41(10), 13100-13104, 2015.
- [4] X. Han, Y. Zhang, C. Zheng, X. Yu, S. Li, W. Wei, "Enhanced Cr(VI) removal from water using a green synthesized nanocrystalline chlorapatite: Physicochemical interpretations and fixed-bed column mathematical model study" *Chemosphere*, 264, 128421, 2021.
- [5] A. Durugkar, S. Tamboli, N.S. Dhoble, S.J. Dhoble, "Novel photoluminescence properties of Eu^{3+} doped chlorapatite phosphor synthesized via sol-gel method" *Materials Research Bulletin*, 97, 466-472, 2018.
- [6] B. Nasiri-Tabrizi, W.J. Basirun, B. Pinguan-Murphy, "Mechanochemical preparation and structural characterization of Ta-doped chlorapatite nanopowders" *Progress in Natural Science*, 26(6), 546-554, 2016.
- [7] J. Wan, C. Zhang, G. Zeng, D. Huang, L. Hu, C. Huang, H. Wu, L. Wang, "Synthesis and evaluation of a new class of stabilized nano-chlorapatite for Pb immobilization in sediment" *Journal of Hazardous Materials*, 320, 278-288, 2016.
- [8] J. Wan, G. Zeng, D. Huang, L. Hu, P. Xu, C. Huang, R. Deng, W. Xue, C. Lai, C. Zhou, K. Zheng, X. Ren, X. Gong, "Rhamnolipid stabilized nano-chlorapatite: Synthesis and enhancement effect on Pb- and Cd-immobilization in polluted sediment" *Journal of Hazardous Materials*, 343, 332-339, 2018.
- [9] S. Subramanian, T.N. Sairam, B.K. Maji, G. Jaiganesh, S.M. Jaya, H. Jena, G. Amarendra, "Lithium uptake in strontium chlorapatite - A combined experimental and first principles study" *Journal of Alloys and Compounds*, 731, 1247-1255, 2018.

- [10] P. Zhai, X. Chen, Z. Zhang, L. Zhu, H. Zhang, W. Zhu, "Facile room-temperature coprecipitation of uniform barium chlorapatite nanoassemblies as a host photoluminescent material" *Particuology*, 37, 37-42, 2018.
- [11] A. Rout, S. Agrawal, "Theoretical and experimental investigation of Gd^{3+} -doped white light emitting chlorapatite $Ca_6Na_2Y_2(SiO_4)_6Cl_2$ synthesized by hydrothermal route" *Indian Journal of Physics*, 96(14), 4143-4154, 2022.
- [12] Q. Yuan, P. Wang, X. Wang, B. Hu, C. Wang, X. Xing, "Nano-chlorapatite modification enhancing cadmium(II) adsorption capacity of crop residue biochars" *Science of the Total Environment*, 865, 161097, 2023.
- [13] T. Kokubo, "Bioactive glass ceramics: properties and applications" *Biomaterials*, 12, 155-163, 1991.
- [14] R. Yu, C. Guo, T. Li, Y. Xu, "Preparation and luminescence of blue-emitting phosphor $Ca_2PO_4Cl: Eu^{2+}$ for n-UV white LEDs" *Current Applied Physics*, 13(5), 880-884, 2013.
- [15] T. Ateş, S. Keser, N. Bulut, O. Kaygılı, "The effects of duration of ultrasonication on the morphology and structural properties of Ni-doped hydroxyapatite structure" *Journal of Physical Chemistry and Functional Materials*, 5 (2), 22-25, 2022.
- [16] B.D. Cullity, "Elements of X-ray diffraction" Addison-Wesley Publishing Company, Massachusetts, 1978.
- [17] O. Kaygılı, S. Keser, "Zr/Mg, Zr/Sr and Zr/Zn co-doped hydroxyapatites: synthesis and characterization" *Ceramics International*, 42(7), 9270-9273, 2016.
- [18] A. Fahami, G.W. Beall, T. Betancourt, "Synthesis, bioactivity and zeta potential investigations of chlorine and fluorine substituted hydroxyapatite" *Materials Science and Engineering: C*, 59, 78-85, 2016.
- [19] O. Kaygılı, S. Keser, M. Kom, N. Bulut, S.V. Dorozhkin, "The effect of simulating body fluid on the structural properties of hydroxyapatite synthesized in the presence of citric acid" *Progress in Biomaterials*, 5, 173-182, 2016.